A Numerical Study of Flow Distribution Effect on a Parallel Flow Heat Exchanger

Kilyoan Chung, Kwan-Soo Lee*
School of Mechanical Engineering, Hanyang University, Seoul 133-791, Korea
Dong-Jin Cha
Department of Building Service Engineering, Hanbat National University, Taejon 305-719, Korea

The effect of flow distribution on thermal and flow performance of a parallel flow heat exchanger has been numerically investigated. The flow distribution has been altered by varying the geometrical parameters that included the locations of the separators, and the inlet/outlet of the heat exchanger. Flow nonuniformities along paths of the heat exchanger, which were believed to be dominantly influential to the thermal performance, have been observed to eventually optimize the design of the heat exchanger. The optimization has been accomplished by minimizing the flow nonuniformity that served as an object function when the Newton's searching method was applied. It was found that the heat transfer of the optimized model increased approximately 7.6%, and the pressure drop decreased 4.7%, compared to those of the base model of the heat exchanger.

Key Words: Flow Distribution, Parallel Flow Heat Exchanger, Flow Nonuniformity, Optimization

Nomenclature

A_{in} : Diameter of inlet(dimensionless, reference lenght)
A_{out} : Diameter of outlet(dimensionless)
b : The width of the header (dimensionless)
C_1, C_2, C_3 : Turbulent model constants
g : Gravitational acceleration, m/s^2
h_e : Equivalent convective heat transfer coefficient, W/m^2 K
H : Enthalpy
k : Turbulence kinetic energy or thermal conductivity, W/mK
L : Length of a PFHE(dimensionless)
l_{in} : Distance from the top of a PFHE to the inlet center
l_{out} : Distance from the bottom of a PHFE to the outler center
$\dot{m}$: Mass flow rate, kg/s
N : Passage number
NP : Number of paths of a model
NPP : Number of passages per path of a model
P : Non-dimensional pressure($=p/0.5\rho u_{in}^2$)
P : Pressure, Pa
P : Pitch(dimensionless)
$\dot{q}$: Heat flux, W/m^2
R_q : Heat flux ratio(dimensionless)
T : Temperature, K

Greek symbols

ε : Turbulent dissipation rate
η : Efficiency
θ : Temperature(dimensionless), $(T-T_{air})/(T_{in}-T_{air})$

Subscripts

air : Ambient air
ave : Average
f : Fin

* Corresponding Author,
E-mail : ksleehy@hanyang.ac.kr
TEL : +82-2-2290-0426; **FAX** : +82-2-2295-9021
School of Mechanical Engineering, Hanyang University, Seoul 133-791 Korea. (Manuscript **Received** April 24, 2001; **Revised** July 31, 2001)

ideal : Ideal case
imp : Improved
in : Inlet
n : Passage index
out : Outlet
psg : Passage
pth : Path
t : Tube
tot : Total

1. Introduction

A parallel flow heat exchanger (PFHE) is quite promising since it has 50% and 40% less volume for same thermal performance than a fine-tube heat exchanger and a serpentine heat exchanger, respectively (Marvillet, 1993). The heat transfer and pressure drop along the refrigerant path play a significant role in determining the overall thermal performance (Sugihara and Lukas, 1990).

The PFHE model in this study is characterized by multiple flow paths and passages (see Fig. 1). Thus, the study must focus on the flow distribution of multiple passages as well as the thermal performance of compact heat exchangers. There have been several studies of flow distribution of multiple passages. Nakamura et al. (1989) designed the passages of a power transformer to using the multi-block method to get uniform flow distribution of air in each passage. Choi et al. (1993) studied the effects of the inlet size of a cooling fan and the spacing between PCB boards on the uniformity of flow distribution, without increase in pumping power, for electronic packaging applications. Sugihara and Lukas (1990) explained the basic structure and materials of a PFHE for automobiles, and some experimental results on its thermal performance were reported.

Despite an abundance of previously published materials on each of pertinent subjects, the results for optimization of compact heat exchangers are very scant. Those for the compact heat exchangers are mostly experimental ones. Although prior works are extremely valuable, they do not provide the extensive database needed for optimization

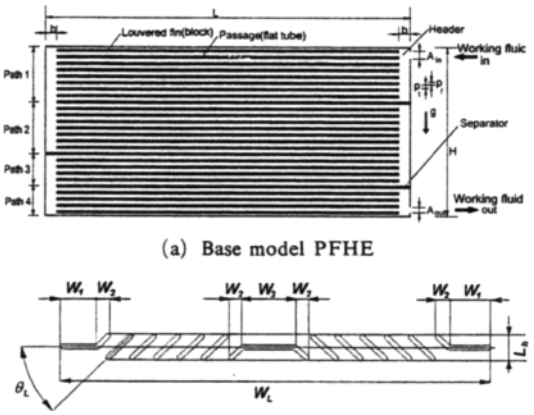

(a) Base model PFHE

(b) Close-up of attached louvered fin

Fig. 1 Schematic diagram of (a) the base model PFHE and (b) close-up of attached louvered fin

study. In particular, the open literature publications dealing with PFHEs are essentially performance evaluations of commercial products.

In this study, the thermal and flow characteristics of a simplified model of a commercial PFHE are numerically analyzed. Some parametric investigations of thermal performance are conducted by varying the geometrical parameters (e. g. locations of the separators, the inlet, and the outlet). The flow nonuniformity, which indicates the dispersion in mass flow rates along the passage in each path, is used for quantifying the thermal performances of the PFHEs. Finally, an optimum technique is applied for suggesting the optimal geometry of the PFHE with maximum thermal performance.

2. Theoretical Analysis

2.1 Mathematical modeling

The PFHE incorporates the passages of the working fluid, plus headers and separators. The passages are usually made up of flat tubes with micro-channels. The dividing header distributes the working fluid into the passages while the combined header collects the fluid from them. The separators determine several different flow paths, each of which has multiple flow passages within it. For improving the airside heat transfer,

Table 1 Principal dimensions of base model geometry with θ_L of 24° (dimensionless)

A_{in}	A_{out}	l_{in}	l_{out}	b
1.00	0.748	1.024	0.866	1.457
H	L	p_t	p_t	
22.677	48.031	0.709	0.157	
W_L	W_1	W_2	W_3	L_h
1.260	0.108	0.108	0.037	0.039

louvered fins are installed between the flat tubes. In this study a PFHE equipped with louvered fins tabulated in Table 1 is simplified into a two-dimensional form for numerical analysis, as shown in Fig. 1. Flow inside the flat tubes of the PFHE is in two-phase. To our knowledge, there is no suitable two-phase flow model reported in the open literature that can be applied to the flow through the tubes of small hydraulic diameter yet. Therefore, a single-phase model is applied instead.

2.2 Governing equations

For the numerical analysis of thermal and flow characteristics of the PFHE, the following assumptions are made;

- two dimensional, steady state, incompressible turbulent flow
- viscosity and density of the working fluid are maintained constant, and
- a flat tube with micro channels in it is considered as a single passage, and the inner surface of the passage is smooth.

Based on the above assumptions, the governing equations are expressed in general coordinates using tensors as follows. The k-ε model is used for a turbulent flow analysis.

$$\frac{\partial}{\partial x_i}(\rho u_i \hat{q}) = \frac{\partial}{\partial x_i}\left(\mu_{eff}\frac{\partial \hat{q}}{\partial x_i}\right) + S_{\hat{q}} \qquad (1)$$

In the governing equation Eq. (1), $\hat{q}$ and source terms for the continuity, u-momentum, v-momentum, energy, and turbulent momentum energy equations are given in Table 2, respectively.

Table 2 $\hat{q}$, $\sigma_{\hat{q}}$, and $S_{\hat{q}}$ used in Eq. (1)

Equations	$\hat{q}$	$\sigma_{\hat{q}}$	$S_{\hat{q}}$
Continuity	1	-	0
x-momentum	u	1.0	$-\partial p/\partial x+\partial/\partial x_i[\mu_{eff}(\partial u_i/\partial x)]$
y-momentum	v	1.0	$-\partial p/\partial y+\partial/\partial x_i[\mu_{eff}(\partial u_i/\partial y)]-\rho g$
Energy	H	0.9	$\partial/\partial x_i[\mu_{eff}(\partial \Delta H/\partial x_i)]$
Turbulent kinematics energy	k	1.0	$\rho(P_r-\varepsilon)$
Turbulent dissipation rate	ε	1.3	$\rho(\varepsilon/k)(C_1P_r-C_2\varepsilon)$

$\mu_{eff}=(\mu+\mu_t)/\sigma_{\hat{q}}$, $\mu_t=\rho C_\mu k^2/\varepsilon$, $C_\mu=0.09$, $C_1=1.44$, $C_2=1.92$

$$P_r=\frac{\mu_t}{\rho}\left[2(u_x^2+v_y^2)+(v_x+u_y)^2-\frac{2}{3}(u_x+v_y)^2\right]$$

2.3 Boundary conditions

The working fluid flows uniformly through the inlet of the PFHE, and there is no mass loss at the inside of the PFHE. The uniform velocity and the mass conservation are imposed as inflow and outflow boundary conditions, respectively. For the inner solid walls of headers and blocks (between the tubes), no-slip conditions are imposed. The headers of the PFHE are exposed to ambient air, and thus, natural convection heat transfer occurs. Forced convection heat transfer by a fan is also produced between the tubes incorporated with louvered fins. For the temperature boundary conditions, the nondimensional temperature at the inlet is set to be unity ($\theta_{in}=1$), while the zero gradient condition is imposed at the outlet. A generalized heat transfer correlation (Chang and Yang, 1997) for the louvered fin geometry is used to determine the value of h. For heat transfer over the blocks, the heat transfer by the louvered fins is also considered, in addition to the one by the tube. Therefore, the overall heat transfer rate q_{tot} can be expressed as follows;

$$\begin{aligned} q_{tot} &= q_t + q_f \\ &= hA_t(T_t - T_{air}) + \eta_f hA_f(T_t - T_{air}) \qquad (2) \\ &= \left(1+\eta_f\frac{A_f}{A_t}\right)hA_t(T_t - T_{air}) \end{aligned}$$

where q_t and q_f are heat transfer rates by the tube and fins, respectively, and A_t, A_f, η_f, T_t, and T_{air} are the tube area, fin area, fin efficiency, surface temperature of tube, and temperature of ambient air, respectively. In Eq. (2) a factor multiplying the heat transfer coefficient, area ratio, and fin efficiency is defined as the equivalent

heat transfer coefficient h_e.

$$h_e=\left(1+\eta_f\frac{A_f}{A_t}\right)h \tag{3}$$

3. Numerical Analysis

The governing equations and associated boundary conditions were discretized by a control-volume finite difference method. A non-staggered grid system was applied for convenience of programming. A checkerboard pressure which often occurred in a non-staggered grid system was treated by adding the 4^{th} order pressure damping term into the pressure correction equation. A predictor/ multi-corrector method was applied to consider the relationship between the velocity and pressure.

The proper size of the grids was determined such that its further increase would not affect much the numerical solution. Four different grid spacing, that was, 5, 10, 12, and 15 mesh lines in each passage, were used to test their effects on numerical results. These led to total grid points of 41,527(=131×317), 59,212(=131×452), 62,749 (=131×479), and 76,897(=131×587), respectively. The corresponding flow distributions were numerically computed. The optimal grid spacing was determined when the solution obtained with a smaller grid spacing showed a negligible improvement in accuracy. It turned out that the 62,749 grid point case produced better flow distribution by 4.7% than the 59,212 grid point case, and that the 76,897 grid point case produced slightly better flow distribution by 0.8% than the 62,749 grid point case. Thus, it was concluded that the case of 12 mesh lines was the optimal value. The results to be discussed are obtained with that grid spacing.

Since there were several regions that did not require computation in the domain, as shown in Fig. 1, a multi-block method (Agrawal et al., 1993) was incorporated for reducing the computation time. The convergences of the iterations for the velocity and temperature were assumed when their changes in iteration were less than 10^{-5}. For flow distribution its change was about 10^{-6}.

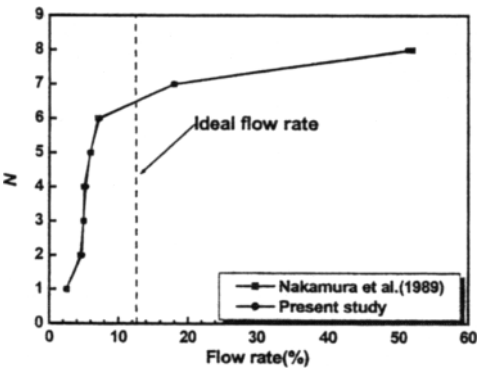

Fig. 2 Comparison of the flow rate with Nakamura et al. (1989)

In order to verify the developed code, a flow field from a multiple passage arrangement that was the same as that described in the reference (Nakamura et al., 1989) was solved by the multi-block method. Figure 2 compares the normalized flow distribution in each path obtained from this study with that given in the reference (Nakamura et al., 1989). As shown in the figure, the two results agree very well, with a maximum deviation of less than 0.3%.

4. Results and Discussions

Thermal and flow characteristics with a base model of PFHE, shown in Fig. 1, and seven modified models have been numerically analyzed. Reynolds number of each model is 9,766 at inlet. All the models are composed of four paths, but the number of passages in each path are different for the different models. For the base model, for example, Paths 1 through 4 have nine, eight, five, and five passages, respectively, as listed in Table 3. Each path and passage has been numbered in ascending order from the top to the bottom. Other changes in the seven models from the base model will be explained shortly.

On completing a computation run with each model, the flow distribution along each path is evaluated, and the flow nonuniformity and heat flux ratio are calculated. The heat transfer as well

Table 3 Passage number in each path for the base model and seven modified models

Model	Passage number (number of tubes)			
	Path 1	Path 2	Path 3	Path 4
Base	1~9(9)	10~17(8)	18~22(5)	23~27(5)
1	1~8(8)	9~15(7)	16~21(6)	22~27(6)
2	1~9(9)	10~17(8)	18~23(6)	24~27(4)
3~7	1~9(9)	10~17(8)	18~22(5)	23~27(5)

as pressure drop between the inlet and outlet are also determined for further comparison. Since the pressure drop for each model is so small, the quantity is normalized by that of the base model and appears as a percentage for the purpose of comparison.

4.1 Flow distribution and nonuniformity

For multiple passage problems, the flow distribution along each path is considered very important (Nakamura et al., 1989; Karvounis and Assanis, 1993; Choi et al., 1993). In general, one of final objectives of the multiple passage problems is to make the flow distribution uniform. Flow along the multiple passages is usually uni-directional. However, all the models in this study consist of several paths divided by the separators and their flow directions alternate. Thus, they are multi-directional rather than uni-directional. For evaluating the degree of flow distribution in paths of each model, the flow nonuniformity FN_{pth}, which indicates the dispersion in mass flow rates along the passages in each path is defined in this study as follows;

$$FN_{pth}=\sqrt{\left\{\sum_{n=N_s}^{N_e}\left(\frac{\dot{m}_{psg,n}-\dot{m}_{psg,id}}{\dot{m}_{psg,id}}\right)^2\right\}\Big/(N_e-N_s)\Big|_{pth}} \quad (4)$$

where N_s and N_e represent passage numbers of the first and last passages of the path being considered, respectively (pth : 1 through 4 in this study). For evaluation of heat transfer rate, we define the heat flux ratio $R\dot{q}_{,pth}$,

$$R\dot{q}_{,pth}=\frac{\dot{q}_{pth}}{\dot{q}_{ave}} \quad (5)$$

where $\dot{q}_{ave}$, the average heat flux in PFHE, is defined as the overall heat transfer rate divided by total heat transfer area while $\dot{q}_{pth}$, the heat flux in each path, is defined as the heat transfer rate in each path divided by the heat transfer area of each path.

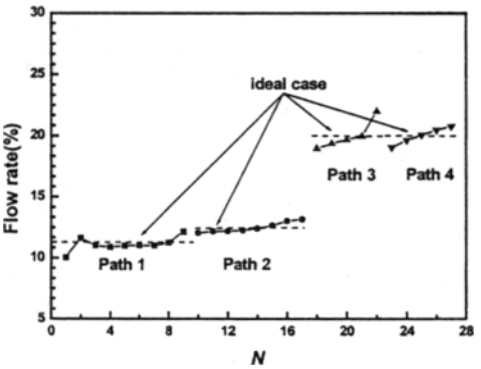

Fig. 3 Flow rates in each path of the base model

Figure 3 shows the flow distribution in each path of the base model. One noticeable trend is that the flow distribution rate at lower passages (larger passage number) is slightly greater than that at upper passages (smaller passage number) for all the paths. This may result from the gravity of the working fluid in the model. Another reason would be the increase of pressure drop between the two headers, distributing and collecting, in lower passages. The pressure drop along each passage is determined by examining the pressure distribution along the vertical mesh lines in the region of the two headers. As expected, the amplitude of the pressure at the distributing header is larger than that at the collecting header. However, the flow distribution for the upper passages of Path 1, as shown in Fig. 3, is different from that of the rest of the paths. That is, the flow rate near Passage 2 is larger than that of the lower passages. This is caused by the location of the inlet; the working fluid that is supposedly distributed to the upper passages evenly flows directly into Passage 2. The smaller flow rate at Passage 1 of Path 1 is also caused by the effect of gravity.

The flow nonuniformity FN_{pth} and heat flux ratio $R\dot{q}_{,pth}$, defined by Eqs. (4) and (5), of all the models are determined, as shown in Table 4. In the base model, flow nonuniformities of Paths 2 and 3 are slightly higher than those of the other

Table 4 FN_{imp}, FN_m, $\Delta\theta$, ΔP, and $R\dot{q}$ of the base model and Models 1~7

Model	NPP, l_{in}, l_{out}	$FN_{imp}(\times 10^3)$				$\Delta\theta/\Delta P$			
		FN_1	FN_2	FN_3	FN_4	$R\dot{q}_{,1}$	$R\dot{q}_{,2}$	$\dot{q}R\dot{q}_{,3}$	$\dot{q}_{,4}$
Base	9-8-5-5, 1.024, 0.866	1.98				0.500/100.0			
		0.04	3.34	4.10	1.16	1.31	0.89	0.87	0.96
1	8-7-6-6, 1.024, 0.866	2.59				0.496/105.3			
		0.01	0.86	9.43	1.23	1.43	1.13	0.71	0.89
2	9-8-6-4, 1.024, 0.866	23.56				0.469/116.5			
		0.04	42.30	48.62	1.38	1.88	0.34	0.31	0.93
3	9-8-5-5, 0.291, 0.866	1.82				0.498/96.7			
		4.15	1.30	0.03	0.26	0.74	0.93	1.26	1.07
4	9-8-5-5, 1.756, 0.866	1.14				0.508/100.4			
		0.85	0.70	3.36	0.16	1.05	1.06	0.76	1.13
5	9-8-5-5, 2.756, 0.866	4.41				0.472/99.8			
		10.54	2.65	0.00	0.57	0.73	0.95	1.31	1.09
6	9-8-5-5, 1.024, 0.331	2.04				0.497/97.4			
		0.02	1.29	4.19	4.73	1.51	0.99	0.84	0.80
7	9-8-5-5, 1.024, 2.189	3.09				0.497/109.4			
		0.08	2.60	9.91	2.45	1.33	0.91	0.83	0.91

two paths, but their heat flux ratios are lower. This may imply that a uniform flow distribution can improve the thermal performance because the opposite may be true. It is thus assumed that the reduction in the flow nonuniformity, which can be obtained by varying geometry of the base model of the PFHE, may improve the overall heat transfer of the PFHE and may further optimize the heat exchanger.

In an effort to improve higher flow nonuniformities of Paths 2 and 3 of the base model, a few of its geometrical parameters of the base model are varied. The selected parameters are all the inner dimensions of the PFHE, that is, the locations of the separators, the inlet, and the outlet.

First, the locations of the separators of the base model are varied, generating two modified models; one is Model 1, having eight-seven-six-six passages for Paths 1 through 4, respectively, and the other is Model 2 having nine-eight-six-four passages. It turned out that neither Model 1 nor Model 2 improved the higher flow nonuniformities of the base model. Actually the results of the two models are worse than those of the base model in terms of flow nonuniformity and heat flux ratio, as listed in Table 4. It was thus concluded that changes in the locations of the separators alone might not improve the thermal performance.

Next, the effects of the inlet and outlet locations on the thermal performance were investigated. The location of inlet (l_{in}) is defined as the distance from the top of the PFHE to the center of inlet and the location of outlet (l_{out}) by the distance from the bottom of the PFHE to the center of outlet. Models 3 through 5 have inlets at different locations as compared to the base model while maintaining the other two parameters the same, as tabulated in Table 4. Similarly, Models 6 and 7 have outlets at different locations with the remaining parameters being the same as those of the base model. The flow distributions of Models 3-7 are shown in Fig. 4.

Model 3 has the inlet between Passages 1 and 2, which is the upper part of Path 1. The fluid flow to Passage 1 increases, compared to that of the base model, resulting in worse FN. On the contrary, for Models 4 and 5, the inlet is lowered and thus the flow rate along Passages 1 and 2 are

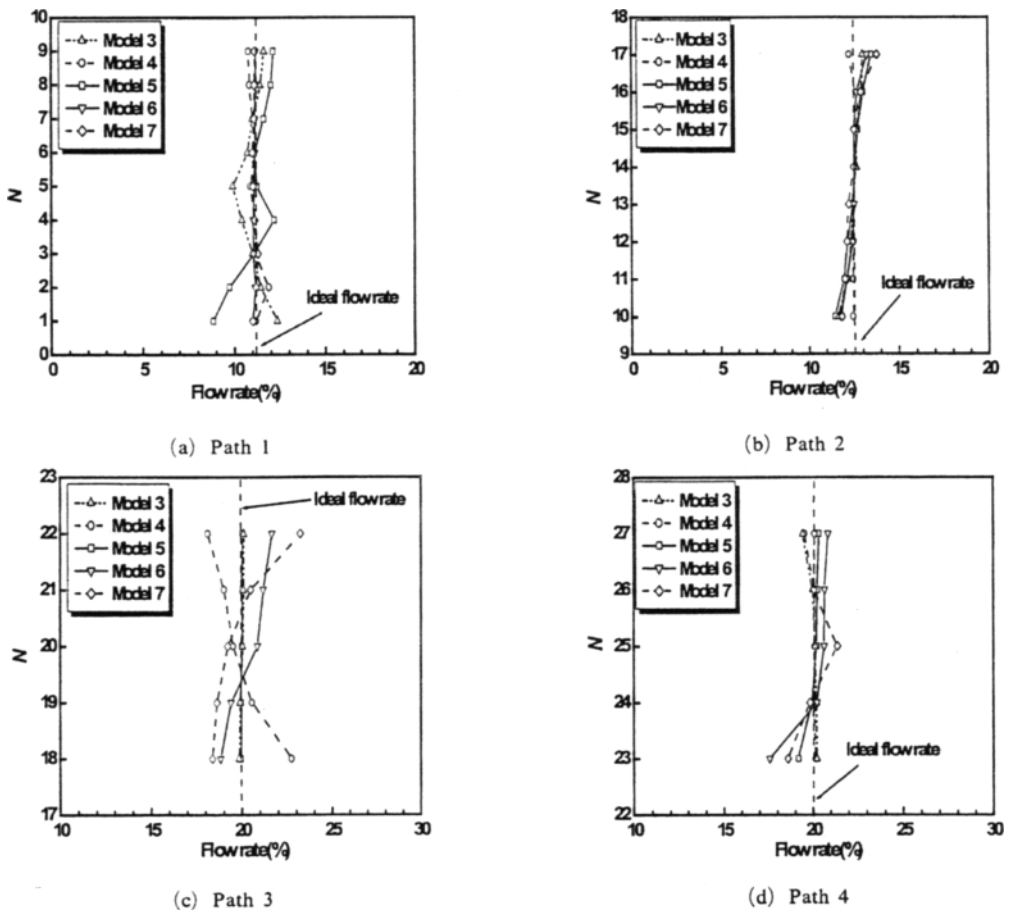

Fig. 4 Flow rates in each path of Models 3-7

smaller, causing worse FN as well. This can be observed more vividly in the case of Model 5. For Model 6, the fluid passing through Passage 27 flows directly to the outlet that is located in the lowest part of Path 4, while the fluid passing through the remaining passages in Path 4 is blocked by the flow stream from Passage 27. Thus, FN_4 is high. FN_4 of Model 7 is also high, and the reason in this case is that the fluid passing through Passages 26 and 27 are stagnated, because the outlet of Model 7 is located above the center of Path 4. The increment in the flow resistance in Path 4 adversely affects even the flow in Path 3. It is observed that FN_3 and FN_4 are worse. From these runs, the FN and heat flux ratio of all the models considered are calculated, as tabulated in Table 4.

4.2 Pressure drops and heat transfer

The results in the previous section indicate that uniform flow distribution over all the passages may provide better thermal performance. During data reduction, however, it is found that the FN in Eq. (4) may not be a good measure for evaluating the thermal performance of the PFHE. Generally, each path of the models has the different number of passages and thus different sizes of heat transfer areas. Supposedly, two paths having different numbers of passages can be considered. However, in case their FN values are the same, it is still possible for them to have different heat flux ratios because of their different heat transfer areas. Therefore, a new flow nonuniformity $FN_{imp,}$, which is basically a modification of the previously defined FN, is defined by considering the ratio of the heat transfer areas as follows;

$$FN_{imp}=\frac{1}{NP}\sum_{m=1}^{NP}\frac{A_m}{A_{tot}}\times FN_{pth} \tag{6}$$

where A_m and A_{tot} represent heat transfer areas of each path and the overall PFHE, respectively. Since the FN_{imp} reflects the difference of the numbers of passages in each path, it is now possible to directly compare thermal performance of each model. With this information, nondimensional outlet temperature and pressure drops of all the models considered are compared, as listed in Table 4. As shown in the table, all the geometrical factors considered (the locations of the separators, the inlet, and the outlet) have influence on the FN_{imp}, in some degree, and the FN_{imp} would determine not only the heat transfer but also the pressure drop of each model. In other words, keeping the FN_{imp} low is for enhancement of heat transfer and for reduction in pressure drop as well.

In general, those models that vary the locations of separators, that is Models 1 and 2, show larger FN_{imp} and worse thermal performance than the base model, as shown in Table 4. This means that a set of parameters NPP in Table 4, which are determined by the locations of separators, would be dominant. In this type of PFHE, however, there are a small number of passages (27), and thus the set of parameters may not be easily adjustable. Thus, the set of parameters keeps fixed as that of the base model and the other two parameters are considered, instead of trying to find other set of parameters that might provide better results.

As previously discussed, for example, the case of Model 5, having the inlet at the upper part of Path 1 results in higher FN_{imp}. Similarly, having outlet at the lower half of Path 4-the case of Model 7-also results in higher FN_{imp}. Among all the models, Model 4 that varies the location of the inlet from the base model shows superior thermal performance in terms of heat transfer and pressure drop to any other models considered. In this study, a correlation of FN_{imp} to other factors is formulated, based on the numerical results. By utilizing the correlation, an optimization of the PFHE could be made in terms of the heat transfer and pressure drop.

5. Optimization

As discussed earlier with the numerical results, an optimization of the PFHE in terms of heat transfer and pressure drop is directly related to the FN_{imp}. In other words, the optimization can be done by finding the parametric values in such a way that the FN_{imp} of the model can be minimized, providing its maximum thermal performance. The FN_{imp} is chosen as an object function in this study. Seven other runs were conducted to generate raw data for the optimization process by varying the locations of the inlet and outlet while the locations of the separators were fixed at 9-8-5-5, and their FN_{imp} were calculated. The data of FN_{imp} are curve-fit by a polynomial function in terms of the location of the inlet l_{in} and the location of the outlet l_{out}, with the unknown coefficients to be found. The correlation of l_{in} and l_{out} could be found with the object function as follows;

$$\frac{1}{l_{in}}=a+b\left(\frac{l_{out}}{1.78}\right)+c\left(\frac{l_{out}}{1.78}\right)^2 \tag{7}$$

where coefficients a, b, and c are 3.04×10^{-1}, -1.7×10^{-2}, and 2.58×10^{-4}, respectively. Using Eq. (7), the FN_{imp} can be expressed as

$$FN_{imp}=2.1215-2.88\times10^{-3}\left[a+b\left(\frac{l_{out}}{1.78}\right)+c\left(\frac{l_{out}}{1.78}\right)^2\right]^{-2.5}+5.4\times10^{-4}\left[a+b\left(\frac{l_{out}}{1.78}\right)+c\left(\frac{l_{out}}{1.78}\right)^2\right]^{-3} \tag{8}$$

Using the second order Newton's searching method, a value of l_{out} for minimum FN_{imp} can be found. The corresponding value of lin can also be found by using Eq. (7). It turned out that those values of l_{in} and l_{out} for the optimization were 1.551 and 0.858, respectively. Another simulation was executed with these optimized values of l_{in} and l_{out}, and the FN_{imp} was found to be 0.807×10^{-3}. This is a lower value than that of any other models considered. $\Delta\theta$ and ΔP for this optimized geometry are 0.538 and 95.30, respectively. This indicates that the heat transfer of the optimized model has been increased approximately 7.6% and the pressure drop decreased 4.7%, compared to

those of the base model.

6. Conclusions

Internal flow and thermal characteristics of the PFHE have been studied to improve its thermal performance. The improved flow nonuniformity FN_{imp}, which is believed to be crucial to the thermal performance of the PFHE, has been introduced to quantify the effects of geometrical parameters of the PFHE. An optimum scheme that can minimize the flow nonuniformity has been developed and investigated with variation of parameters by employing the Newton's searching method. When the PFHE model is optimized, it can reduce the pressure drop by 4.7% and increase the heat transfer by 7.6%, compared to those of the base model.

Acknowledgement

The authors would like to thank the Ministry of Science and Technology, Korea, for the financial support by a grant from the Critical Technology 21 Project and BK21 project.

References

Agrawal, A. K., Krishnan, S., and Yang, T., 1993, "Use of Subdomains for Inverse Problems in Branching Flow Passages," *ASME J. of Fluids Eng*. Vol. 115, pp. 227~232.

Chang, Y. J., and Wang, C. C., 1997, "A Generalized Heat Transfer Correlation for Louvered Fin Geometry," *Int. J. Heat Mass Transfer*, Vol. 40, No. 3, pp. 533~544.

Choi, S. H., Shi, S.. and Cho, Y. I., 1993, "The Effect of Area Ratio on the Flow Distribution in Liquid Cooling Module Manifolds for Electronic Packaging," *Int. Comm. Heat Mass Transfer*, Vol. 20, pp. 221~234.

Karvounis, E. and Assanis, D. N., 1993, "The Effect of Inlet Flow Distribution on Catalytic Conversion Efficiency," *Int. J. of Heat Transfer*, Vol. 36, No. 6, pp. 1495~1504.

Marvillet, C., 1993, "Recent Developments in Heat Exchangers for Automotive Applications," *Recent Developments in Finned Tube Heat Exchangers Theoretical and Practical Aspects*, DTI, Energy Tech, Denmark, pp. 8~51.

Nakamura, Y., Jia, W., and Yasuhara, M., 1989, "Incompressible Flow through Multiple Passages," *Numer. Heat Transfer*, Vol. 16, pp. 451~465.

Sugihara, A. and Lukas, H. G., 1990, "Performance of Parallel Flow Condensers in Vehicular Applications," *SAE Technical Paper Series* 900597, pp. 1~16.